Journal of Applied Polymer Science

Cr(III)-Containing Fe_3O_4/Mercaptopropanoic Acid-Poly(2-hydroxyethyl acrylate) Nanocomposite: Highly Active Magnetic Catalyst for Direct Hydroxylation of Benzene

Farzad Zamani,[1,2] Sahar Kianpour,[1] Behshad Nekooei[2]

[1]Laboratory of Applied Chemistry, Central Laboratory Complex, Isfahan Science and Technology Town, Isfahan University of Technology, Isfahan 8415683111 Iran

[2]Department of Chemistry, Shahreza Branch, Islamic Azad University, Shahreza 31186145 Isfahan, Iran

Correspondence to: F. Zamani (E-mail: fzamani@iaush.ac.ir)

ABSTRACT: In this study, polymer-grafted magnetic nanoparticles containing chromium(III) ions incorporated onto Fe_3O_4/mercaptopropanoic acid-poly(2-hydroxyethyl acrylate) was prepared via a simple and *in situ* method. The obtained magnetic nanocomposite exhibited high catalytic activity and excellent selectivity in direct hydroxylation of benzene in the presence of hydrogen peroxide under solvent-free condition. The magnetic catalyst could be also separated by an external magnet and reused seven times without any significant loss of activity/selectivity. Due to the Lewis acidity of the Fe^{3+} groups in the structure of magnetic nanoparticles, the high efficiency of this catalyst is possibly due to the synergetic effect of Cr^{3+} and Fe^{3+} groups in the structure of magnetic nanocomposite. © 2014 Wiley Periodicals, Inc. J. Appl. Polym. Sci. **2014**, *131*, 40383.

KEYWORDS: catalysts; composites; grafting; magnetism and magnetic properties; properties and characterization

Received 8 October 2013; accepted 1 January 2014

DOI: 10.1002/app.40383

INTRODUCTION

Phenol is an important industrial feedstock and is widely used in the production of phenol resins, fibers, dyestuffs, and medicaments.[1] Industrially, more than 90% of the world's phenol production is based on the three-step cumene (isopropylbenzene) process. However, this method suffers from many disadvantages such as using a large amount of inorganic acid as catalyst, producing a high amount of acetone as byproduct, low reaction yield/selectivity, and harsh reaction conditions. In order to overcome these drawbacks, the one-step hydroxylation of benzene is a good alternative even though this reaction is one of the most difficult in the field of organic synthesis. Over the last decade, they have been reported that transition metal catalysts in the presence of H_2O_2 as a green oxidant exhibit high catalytic activity in the direct hydroxylation of benzene under relatively mild reaction conditions.[2–5] Therefore, synthesis of phenol by direct hydroxylation of benzene in liquid phase over transition metal oxide catalysts using hydrogen peroxide has become attractive in both academic and industrial fields, due to positive effects in terms of cost, safety, and environmental impact.

Over the last few years, magnetic nanoparticles (e.g., Fe_3O_4) have been extensively investigated as inorganic support for the synthesis of organic–inorganic hybrid materials, due to their potential applications in many industrial and biological fields.[6] Their magnetic character implies that they respond to a magnet, making sampling, and collection easier applications. In addition, when magnetic nanoparticles are used as supports, the size of the support materials is decreased to the nanometer scale, and all of the catalytic sites on the external surface of the particles can be accessible to the substrates.[7] As a consequence, the activity of these nanoparticle-supported catalysts could be improved compared with conventional heterogeneous catalysts based on porous support matrices, where internal pore diffusion in the porous catalysts can represent a rate limiting step.[7] In this way, organic–inorganic hybrid materials based on magnetic nanoparticles have been widely used in the field of biology, medicine, and catalysis.[8–11]

In recent years, modified magnetic nanoparticles have received a lot of attention as support for incorporation of different transition metal ions. However, most of these techniques require many reaction steps to introduce functional groups to the magnetic surface and/or they use organosilica precursors as organic shell in order to prepare a suitable support for trapping the metal ions.[12–16] The organosilane precursors not only involve complicated synthesis and purification method but also are very expensive and toxic. Therefore, from both environmental and economic point of views, preparation of the modified magnetic nanoparticles via a simple method and without using

organoalkoxysilane compounds is highly desirable. In addition, although many research works have been recently reported that Fe_3O_4-containing catalysts have high catalytic performance in the hydroxylation of benzene to phenol,[1,17,18] application of transition metal catalysts based on modified magnetic nanoparticles as heterogeneous catalysts in the direct hydroxylation of benzene has received no considerable attention.

In continuing our efforts toward the development of efficient and environmentally benign heterogeneous catalysts,[19–21] herein, Fe_3O_4/mercaptopropanoic acid-poly(2-hydroxyethyl acrylate) nanocomposite containing Cr^{3+} ions (Fe_3O_4/MPA-PHEA-Cr) was prepared via a simple method as a novel heterogeneous magnetic catalyst, without using organosilane precursors. The main goal of this catalytic synthesis was to introduce a novel and efficient transition metal catalyst based on polymer-grafted magnetic nanoparticles to expand the use of these types of nanocomposites for catalytic oxidation reactions. In order to investigate the catalytic activity of this magnetic catalyst, the direct hydroxylation of benzene was chosen as an important organic reaction in both academic and industrial fields.

EXPERIMENTAL

Catalyst Preparation

The procedure for preparing the Fe_3O_4/MPA-PHEA-Cr nanocomposite includes three steps. The detailed procedure was described as the following:

In the first step, MPA-coated Fe_3O_4 nanoparticles was synthesized by a co-precipitation method as reported previously.[22] $FeCl_3{\cdot}6H_2O$ (13 g) and $FeCl_2{\cdot}4H_2O$ (4.8 g) were dissolved in 100 mL deionized water and stirred at 40°C for 15 min under nitrogen atmosphere. Then, 8 g of MPA were added to the above mixture and PH was adjusted to 11 with NH_4OH solution (25 wt %). The suspension was then refluxed for 6 h under nitrogen atmosphere with vigorous stirring. Finally, the obtained nanocomposite was separated from the aqueous solution by magnetic decantation, washed several times with deionized water, and then dried in a vacuum oven overnight to obtain Fe_3O_4/MPA. For the next step of the preparation of catalyst, the amount of sulfur content of Fe_3O_4/MPA is necessary. Sulfur content of the nanocomposite was estimated by back titration using NaOH (0.1*M*). The known amount of the catalyst was stirred in HCl (0.5*M*) for 30 min. Then, the mixture was filtrated and titrated with NaOH (0.1*M*). Sulfur content of catalysts was found to be 1.3 mmol/g.

In the second step, telomerization of PHEA on the surface of Fe_3O_4/MPA was accomplished by an *in situ* polymerization method. Briefly, 0.4 g of Fe_3O_4/MPA was suspended in 10 mL toluene for 15 min using a sonicator to achieve good dispersion. The mixture was then purged with nitrogen and 2-hydroxyethyl acrylate (HEA, 1.2 mL, 10.4 mmol, the molar ratio of HEA/MPA = 20) were added to the reaction mixture, followed by the addition of azobisisobutyronitrile (AIBN) (0.017 g, 0.1 mmol) drop by drop. Immediately, the flask was immersed in an oil bath at 90°C and the reaction mixture was stirred under nitrogen atmosphere for 12 h. At the end of the reaction, the polymerization was stopped by quenching the flask in an ice bath, and the reaction mixture was diluted with tetrahydrofuran (THF), followed by precipitation in 200 mL hexane. The obtained materials were redispersed in 10 mL of THF and centrifuged to remove any free PHEA homopolymer in order to exclusively obtain PHEA grafted magnetic nanocomposite. Finally, the precipitates were dried in a vacuum oven at 40°C for 24 h to yield Fe_3O_4/MPA-PHEA.

In the third step, incorporation of chromium ions onto the Fe_3O_4/MPA-PHEA nanocomposite was carried out using various amounts of $CrCl_3{\cdot}6H_2O$ (2, 3, 4, and 5 mmol). In a typical reaction, a flask containing a stirred suspension of chrome(III) chloride hexahydrate in 15 mL of dry methanol was purged with nitrogen and heated to 40°C under a nitrogen atmosphere. Fe_3O_4/MPA-PHEA (1 g) was then added in one portion and the resulting suspension was refluxed in a nitrogen atmosphere under vigorous stirring for 6 h. Afterward, the synthesized nanocomposite (Fe_3O_4/MPA-PHEA-Cr) was separated from the suspension by magnetic decantation, washed several times with deionized water and dry methanol, and dried under vacuum at room temperature. The Cr content of the nanocomposite, as determined by atomic absorption spectrometer, was found to be 1.28, 1.87, 2.45, and 2.49 mmol/g for 2, 3, 4, and 5 mmol of used chrome(III) chloride hexahydrate, respectively.

Apparatus

The crystalline structures of the samples were evaluated by X-ray diffraction (XRD) analysis on a Bruker D8 Advance diffractometer with CuK_α radiation at 40 kV and 20 mA. Fourier transform infrared (FTIR) spectra were recorded with a Perkin Elmer 65 spectrometer in the range of 400–4000 cm^{-1}. Transmission electron microscopy (TEM) analysis was performed on a Phillips CM10 microscope at an accelerating voltage of 200 kV. Dynamic light scattering (DLS) was recorded on a HORIBA-LB550. Magnetization measurements were carried out on a BHV-55 vibrating sample magnetometer (VSM). Thermal stability of the catalyst was investigated by thermogravimetric analysis (TGA, TSTA Type 503) at a heating rate of 10°C/min under nitrogen atmosphere. Scanning electron microscopy (SEM) was performed on a Philips XL30 with SE detector. Surface composition was investigated using an X-ray Photoelectron Spectroscopy (XPS) (Thermo VG Multilab 2000) in an ultra-high vacuum with Al Kα radiation.

General Procedure for Direct Hydroxylation of Benzene

The catalytic hydroxylation of benzene using 30% H_2O_2 solution as an oxidant was carried out in a two-necked round-bottom flask. In a typical hydroxylation process, a mixture of catalyst (Fe_3O_4/MPA-PHEA-Cr, 0.03 g) and benzene (0.56 mL, 3 mmol) was placed in a round-bottom flask. Then, a certain amount of H_2O_2 (30%, the molar ratio of benzene/H_2O_2 = 1/2) was added dropwise and the reaction mixture was stirred in the absence of solvent for 1 h. Finally, the magnetic catalyst was separated by an external magnet and the resulting solution was analyzed by off-line GC (Varian CP3800). An internal standard material 1,4-dioxane was used to the quantitatively analysis. The products were also analyzed by gas chromatography-mass spectrometry (GC-MS) (Agilent Technologies 6890 N Network GC system and 5973 Mass selective Detector), especially for any product species which

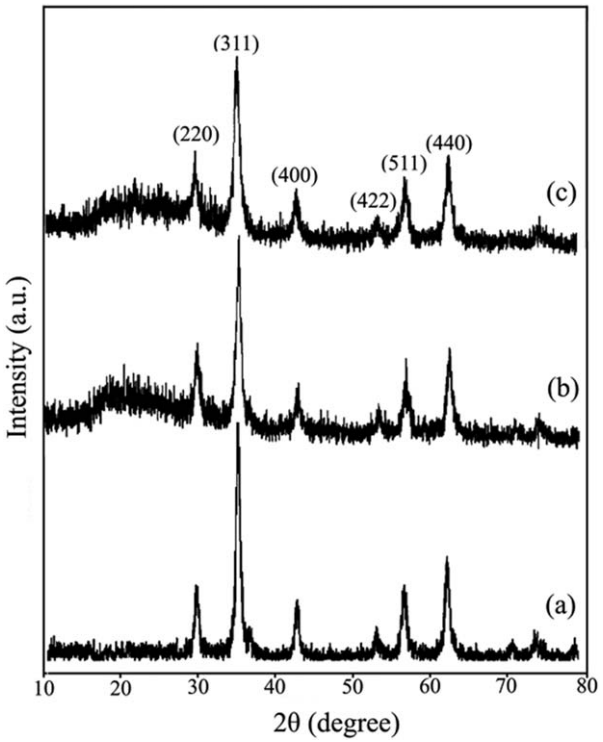

Figure 1. XRD patterns of (a) Fe_3O_4/MPA, (b) Fe_3O_4/MPA-PHEA, and (c) Fe_3O_4/MPA-PHEA-Cr.

cannot be detected by the flame ionization detector (FID) detector. For work-up the reaction mixture, after separation and washing the catalyst with acetonitrile, 5 mL aqueous solution of NaOH (5 wt %) was added and the organic layer was extracted with diethyl ether. Then, 5 mL aqueous solution of HCl (5 wt %) was added to the aqueous layer and the organic layer was extracted with diethyl ether. The solvent of the organic layer was evaporated to afford the pure product.[23]

RESULTS AND DISCUSSION

Catalyst Characterization

Crystalline structures of the Fe_3O_4/MPA, Fe_3O_4/MPA-PHEA and Fe_3O_4/MPA-PHEA-Cr were analyzed by powder XRD. As displayed in Figure 1(a–c), all the samples represent the diffraction peaks at 2θ of around 30.1°, 35.2°, 43.1°, 53.5°, 57.4°, and 62.7° corresponding to the spinel structure of Fe_3O_4,[24] which can be assigned to the diffractions of the (220), (311), (400), (422), (511), and (440) faces of the crystals, respectively. In addition, the XRD patterns depict similar diffraction peaks which indicate that the nanocomposite was synthesized without damaging the crystal structure of Fe_3O_4 core. In addition, the broad diffraction peak in the range of 2θ between 20° and 30° can be attributed to the amorphous polymer coated on the magnetic nanoparticles.[25] According to the XRD results, it can be concluded that the Fe_3O_4 nanoparticles were successfully coated with the MPA-PHEA.

The FTIR spectra of Fe_3O_4/MPA, Fe_3O_4/MPA-PHEA, and Fe_3O_4/MPA-PHEA-Cr nanocomposites were recorded to confirm the modification of the magnetite surface with the organic polymer shell and metal ions [Figure 2(a–c)]. The presence of magnetite nanoparticles is observable by the strong adsorption band at about 585 cm^{-1}, corresponding to the Fe—O vibrations [Figure 2(a–c)]. It is also clear that the strong C=O band of carboxyl group, which is generally present at 1650 cm^{-1}, was absent in the spectrum of Fe_3O_4/MPA [Figure 2(a)]. Instead, two characteristic bands appeared at 1588 and 1514 cm^{-1}, which can be ascribed to COO^-_{as} and COO^-_{s} stretch of carboxyl group.[22] It has been reported that the wavenumber separation between the COO^-_{as} and COO^-_{s} IR bands can be used to distinguish the type of the interaction between the carboxylate head and the metal atom.[26] Because the wavenumber separation between the COO^-_{as} and COO^-_{s} bands is 74 cm^{-1} (1588–1514 = 74 cm^{-1}), it can be concluded that the interaction between the COO^- group and the Fe atom was covalent and bidentate [Figure 2(a)].[26] According to the Figure 2(a), successful Fe_3O_4 surface modification with MPA moieties were verified. The presence of peaks at around 2800–3000 cm^{-1} and ~685 cm^{-1} also corresponds to the aliphatic C—H stretching of the methylene groups and the stretching vibration of C—S band, which is observable in the samples [Figure 2(a–c)]. Looking more closely at the Figure 2(a,b), it can be seen that the peak at 2581 cm^{-1} attributing to the S—H stretches [Figure 2(a)] disappeared in the spectrum of Fe_3O_4/MPA-PHEA, which indicate that SH groups (free thiol groups) in the structure of MPA were reacted with the monomer (HEA) and PHEA was anchored to the surface of Fe_3O_4/MPA through the thiol groups. Moreover, the presence of the polymer (PHEA) on the surface of magnetic nanocomposite (Fe_3O_4/MPA) can be further proved by the appearance of new bands at 3476, 1732, and 1165 cm^{-1} which are due to the stretching vibrations of O—H, C=O, and C—O bonds [Figure 2(c)]. In terms of the Fe_3O_4/MPA-PHEA-Cr [Figure 2(c)], a red shift of the band at 1732 cm^{-1} was observed (1732 cm^{-1} → 1703 cm^{-1}), which is probably characteristic of the asymmetrical fluctuations of the carbonyl group after interaction with the metal ions. The band 3476 cm^{-1} corresponding to the O—H bond of PHEA [Figure 2(b)], disappeared in the spectrum of the Fe_3O_4/MPA-PHEA-Cr [Figure 2(c)], indicating a strong interaction between the oxygen donors and the metal

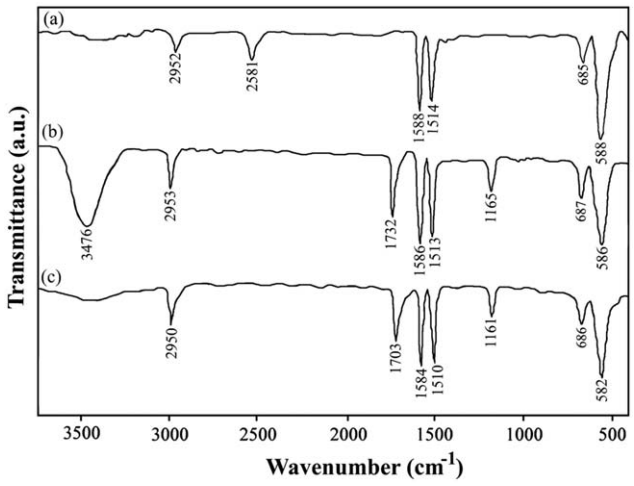

Figure 2. FTIR spectra of (a) Fe_3O_4/MPA, (b) Fe_3O_4/MPA-PHEA, and (c) Fe_3O_4/MPA-PHEA-Cr.

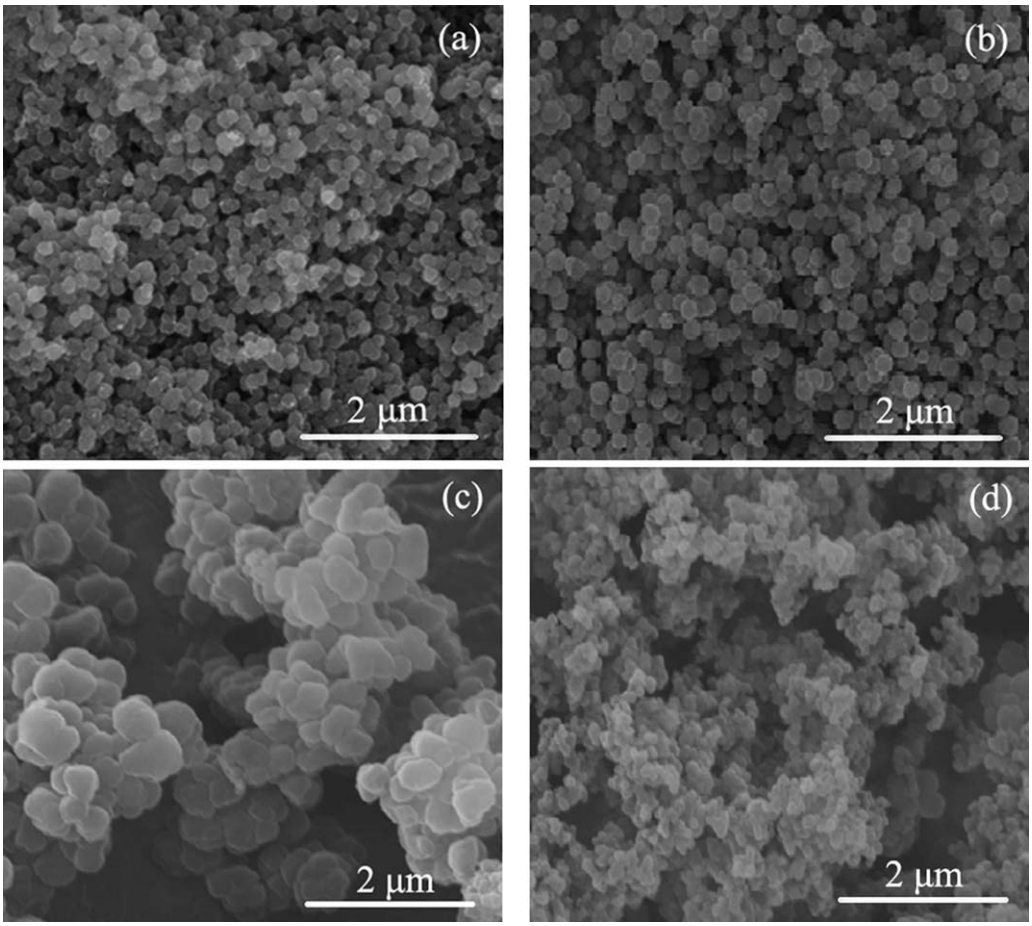

Figure 3. SEM micrographs of (a) Fe_3O_4, (b) Fe_3O_4/MPA, (c) pure PHEA, and (d) Fe_3O_4/MPA-PHEA.

ions. The IR results imply that MPA-PHEA-Cr was successfully immobilized onto the surface of magnetic nanoparticles.

Figure 3 shows the SEM images of Fe_3O_4, Fe_3O_4/MPA, pure PHEA, and Fe_3O_4/MPA-PHEA magnetic nanocomposite. As can be seen, Fe_3O_4 and Fe_3O_4/MPA samples have roughly spherical morphology [Figure 3(a,b)]. No apparent change in the morphology of Fe_3O_4 nanoparticles was observed after modifying with MPA, which is suitable for immobilization of the polymer. The apparent physical nature of PHEA [Figure 3(c)] changed remarkably after composite formation. The nanocomposite [Figure 3(d)] depicts a much smaller of the particle size than that of PHEA microparticles [Figure 3(c)] synthesized in the same conditions without Fe_3O_4 nanoparticles. It can be explained that the MPA grafted on the surface of Fe_3O_4 nanoparticles is good compatible with PHEA. Therefore, the PHEA are polymerized easily and adhered on the surface of Fe_3O_4 nanoparticles instead of forming separate polymer particles. Moreover, the Fe_3O_4 nanoparticles acted as a crystal nucleus for the easier precipitation of PHEA, leading to form the smaller particles.[27] In other words, MPA-modified magnetic nanoparticles serve as not only an inorganic filler but also an effective stabilizer for the polymerization of HEA in the reaction mixture.

To ascertain the composite morphology more clearly, the TEM images of Fe_3O_4/MPA and Fe_3O_4/MPA-PHEA-Cr nanocomposites were represented in Figure 4. Comparison of the TEM micrographs confirms that the original size and shape of the magnetic nanoparticles were retained after grafting of MPA-PHEA-Cr [Figure 4(a,b)]. The composite particles that were obtained by our procedure are quasi-spherical in shape, in which Fe_3O_4 nanoparticles were well dispersed in the polymer matrix. It is also clear from Figure 4(b) that the magnetic nanoparticles are visible as dark contrast areas with uniform dispersion, whereas the MPA-PHEA-Cr shell formed fringes surrounding the magnetic nanoparticles cores. DLS measurements were also carried out to measure the hydrodynamic diameter of the magnetic nanoparticles. Before the surface grafting by PHEA, the mean diameter of the modified-magnetic nanoparticles (Fe_3O_4/MPA) was found to be about 20 nm [Figure 4(c)]. The size of Fe_3O_4/MPA-PHEA-Cr became larger than the Fe_3O_4/MPA because of the grafting of PHEA-Cr on the surface of Fe_3O_4/MPA nanoparticles and was observed to be around 25 nm [Figure 4(d)].

Figure 5 depicts the TGA results of pure PHEA, Fe_3O_4/MPA, and Fe_3O_4/MPA-PHEA nanocomposite under nitrogen atmosphere. It is observed that the Fe_3O_4/MPA loses about 15% of its total weight because of removal the grafted-MPA on the Fe_3O_4 nanoparticles [Figure 5(a)]. In comparison with the Fe_3O_4/MPA, the TGA curve of Fe_3O_4/MPA-PHEA represents a major decomposition at the temperature range from around 250°C to

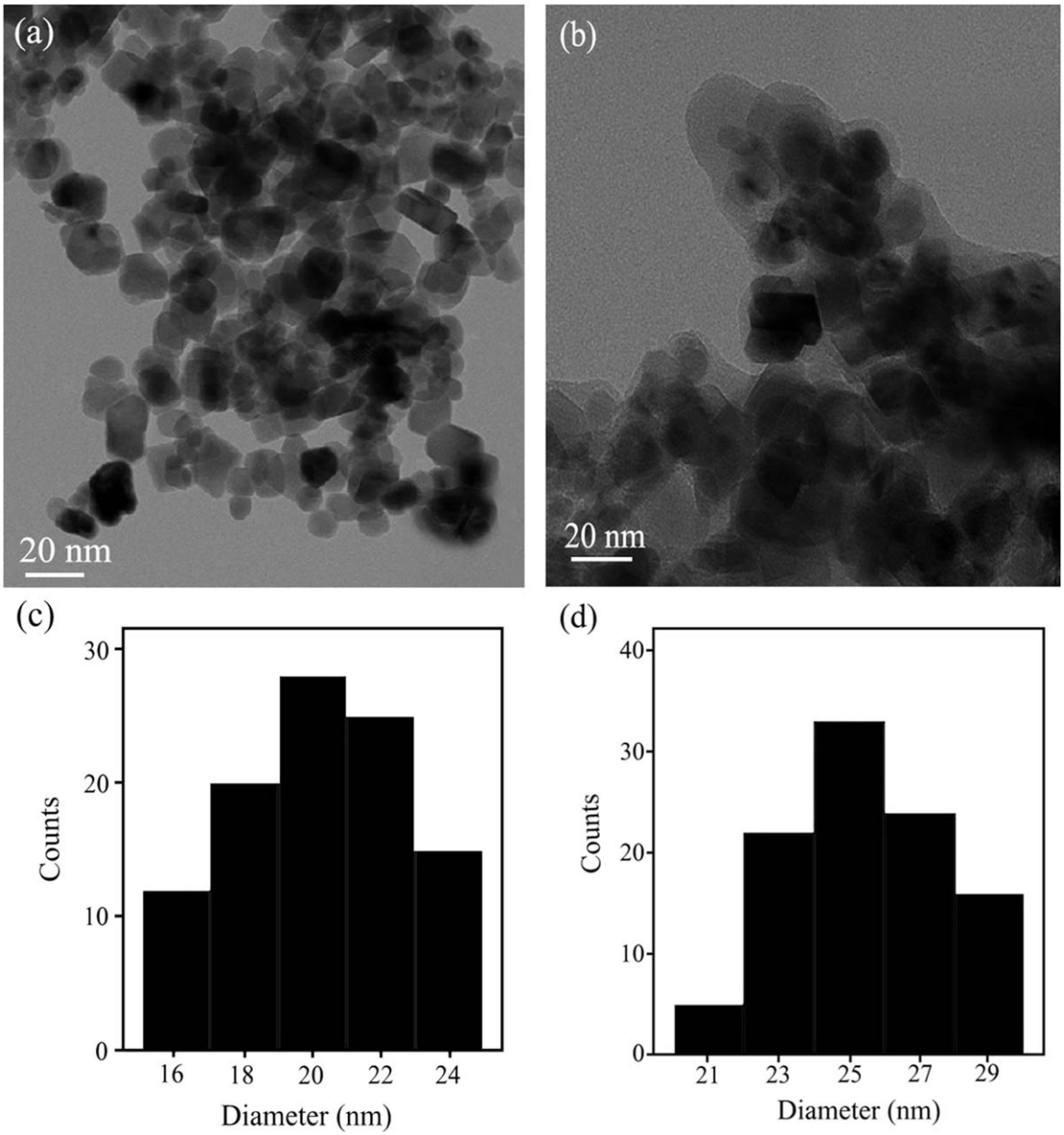

Figure 4. TEM images and the size distributions of (a, c) Fe_3O_4/MPA and (b, d) Fe_3O_4/MPA-PHEA-Cr.

420°C indicating the surface grafting of Fe_3O_4 nanoparticles by MPA-PHEA, which is observed to be ~75% [Figure 5(b)]. TGA results also suggest that Fe_3O_4/MPA-PHEA nanocomposite has higher thermal stability than the pure PHEA [Figure 5(a)], which is possibly due to chemically bonded of PHEA to the surface of Fe_3O_4/MPA nanoparticles and exhibit a relatively high stability.

The magnetic properties of the calcined Fe_3O_4/MPA-PHEA (calcined at 600°C for 3 h), uncalcined Fe_3O_4/MPA-PHEA, and Fe_3O_4/MPA-PHEA-Cr nanocomposite were measured via VSM at room temperature [Figure 6(a–c)]. It can be seen that the saturation magnetization (Ms) value of the samples are 61.8, 38.2, and 32.6 emu/g for the calcined Fe_3O_4/MPA-PHEA, uncalcined Fe_3O_4/MPA-PHEA, and Fe_3O_4/MPA-PHEA-Cr nanocomposite, respectively. As displayed in the figure, the Ms of uncalcined nanocomposite [Figure 6(b)] is significantly less than that of the calcined nanocomposite [Figure 6(a)]. It may be attributed to the fact that the Fe_3O_4 nanoparticles were coated completely by an inert organic shell (MPA-PHEA), which ensures the magnetic nanoparticles with protection and stabilization, avoiding oxidation in air. From the results of the magnetic properties and TEM analysis, the presence of MPA-PHEA around the Fe_3O_4 nanoparticles can be further proved.

In order to investigate the oxidation state of Cr in the nanocomposite, the XPS study was carried out on the Fe_3O_4/MPA-PHEA-Cr catalyst (Figure 7). The high-resolution Cr 2p

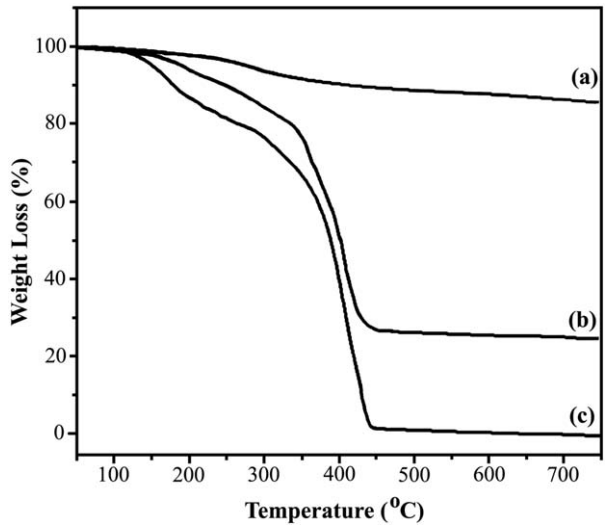

Figure 5. TGA curves of (a) Fe_3O_4/MPA, (b) Fe_3O_4/MPA-PHEA, and (c) pure PHEA.

spectrum exhibits two main peaks at 584.7 and 575.5 eV which are attributed to Cr $2p_{1/2}$ and Cr $2p_{3/2}$, respectively. In comparison with the standard binding energy of Cr(III) at 587.2 eV and 577.7 eV for Cr $2p_{1/2}$ and Cr $2p_{3/2}$, respectively,[28] it can be seen that the Cr peaks in the Fe_3O_4/MPA-PHEA-Cr shifted to lower binding energy. It has been reported that the position of metal peak in the XPS analysis is usually influenced by the local chemical/physical environment around metal species besides the formal oxidation state, and shifts to lower binding energy when the charge density around it increases.[29] Therefore, it can be concluded that Cr(III) ions bound directly to oxygen groups in the structure of polymer supported onto the magnetic nanoparticles in which the charge density around the metal ions increases, which is in agreement with IR results.

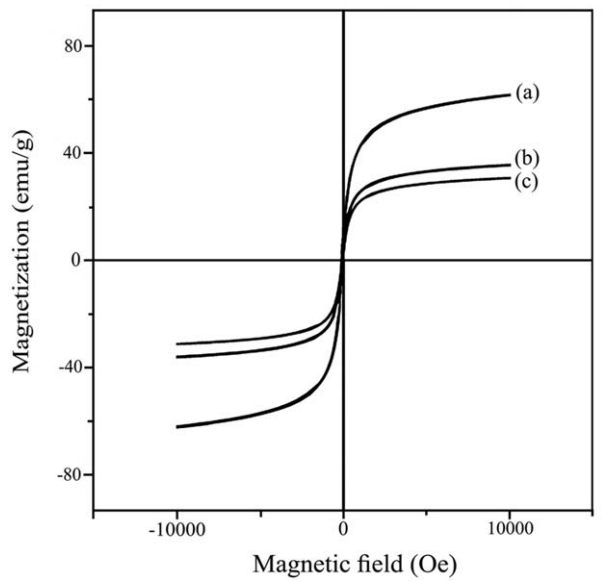

Figure 6. Room temperature magnetization curves of (a) calcined Fe_3O_4/MPA-PHEA nanocomposite (at 600°C for 3 h), (b) uncalcined Fe_3O_4/MPA-PHEA nanocomposite, and (c) Fe_3O_4/MPA-PHEA-Cr nanocomposite.

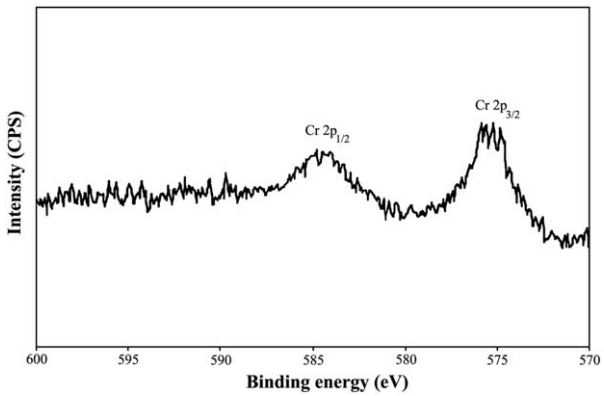

Figure 7. High-resolution XPS spectrum of Cr 2p of Fe_3O_4/MPA-PHEA-Cr nanocomposite.

Catalytic Activity

Having synthesized and characterized the Fe_3O_4/MPA-PHEA-Cr nanocomposite, its role as a heterogeneous catalyst was evaluated for direct hydroxylation of benzene in the presence of hydrogen peroxide as an oxidant. In order to optimize the reaction conditions and obtain the best catalytic activity, different reaction parameters such as solvent, temperature, and amount of catalyst and oxidant were investigated. The hydroxylation reactions of benzene were carried out over the catalyst with the best metal content (reported in the "Experimental" section, 2.45 mmol/g).

As far as the amount of oxidant is concerned, the model reaction was carried out in different amounts of H_2O_2 to investigate the efficiency of the catalyst (Table I). As can be seen, the yield of phenol increased from 8% to 14% with the increase in H_2O_2 amount from 3 to 6 mmol. With further increase in the amount of H_2O_2, the yield decreased, which may be due to the possibility of blocking active sites of the catalyst by water molecules from H_2O_2 solution.[30] In addition, the selectivity to phenol decreased by an increase in the amount of H_2O_2 because of the further oxidation of phenol with excess H_2O_2.

In order to further optimize reaction conditions, the model reaction was performed in several solvents as well as solvent-free condition (Table II). It was observed that the best yield was obtained when the reaction was conducted under solvent-free condition (14%). Moreover, the effect of catalyst amount on the hydroxylation benzene was also investigated by different amounts of the catalyst (Table II). As can be seen, while the amount of catalyst surged from 0.01 to 0.03 g, the product yield raised significantly from 14% to 31%, which is probably due to the availability of more acid sites. Since then, the percentage of yield further increased between 0.03 g and 0.05 g, with a reduction in phenol selectivity from 100% to 79% due to over-oxidation of the substrate at high amounts of the catalyst. According to the results, 0.03 g was chosen as the optimum amount of catalyst, due to the best yield and selectivity, for the further steps.

Table I. Effect of Oxidant Amount on Hydroxylation of Benzene[a]

Amount of H_2O_2 (mmol)	Yield (%)[b]	Selectivity to phenol (%)
3	8	100
6	14	100
9	19	93[c]
12	10	81[c]

[a] Reaction conditions: benzene (3 mmol), catalyst (Fe_3O_4/MPA-PHEA-Cr, 0.01 g), solvent-free, room temperature, reaction time = 1 h.
[b] Isolated yield.
[c] Determined by GC. The main byproduct was quinone.

The influence of reaction temperature on the catalytic activity was investigated by several separate reactions under the same reaction conditions. As represented in Table III, the reaction yield raised by increasing the temperature to 45°C and then it decreased at higher temperatures because of the spontaneous decomposition of H_2O_2 to O_2 and H_2O at high temperatures.[31] Furthermore, it was seen that selectivity to phenol decreased with an increase in the reaction temperature because of the further oxidation of phenol at high temperatures. According to the results, room temperature appears to be the optimum reaction temperature.

It should be mentioned that in order to better understand the active sites of the catalyst, the optimized hydroxylation of benzene was performed in the presence of Fe_3O_4 nanoparticles (purchased from Aldrich, catalog No: 637106) and pure PHEA-Cr separately. The product yields of 6% and 12% were obtained in 240 min and 180 min for Fe_3O_4 and PHEA-Cr, respectively. Furthermore, the selectivity to phenol was not satisfying, 38% and 42% for Fe_3O_4 and PHEA-Cr, respectively. It is clear that apart from the magnetic property of Fe_3O_4 nanoparticles, they have the Lewis acid property. In other words, Fe^{3+} species in the magnetic nanoparticles are capable of catalyzing the hydroxylation reaction. Therefore, the high efficiency of this magnetic catalyst (Fe_3O_4/MPA-PHEA-Cr) could be due to the synergetic effect of Cr^{3+} ions and Lewis acidity of the Fe^{3+} groups in the structure of magnetic nanocomposite, which facilitate the formation of product intermediate. Hence, gathering evidences from all these, the conclusion can be made that the Fe^{3+} groups, which are present in the nanocomposite, have a supplement role in the catalytic activity.[32]

Table II. Effect of Different Solvents and Amounts of Catalyst on the Hydroxylation of Benzene in the Presence of Fe_3O_4/MPA-PHEA-Cr[a]

Solvent	Catalyst (g)	Amount of Cr^{3+} (mmol)[b]	Yield (%)[c]	Selectivity to phenol (%)
CH_3CN	0.01	0.0245	10	100
H_2O	0.01	0.0245	3	100
CH_3OH	0.01	0.0245	5	100
CH_2Cl_2	0.01	0.0245	8	100
Solvent-free	0.01	0.0245	14	100
Solvent-free	0.02	0.0490	26	100
Solvent-free	0.03	0.0735	31	100
Solvent-free	0.04	0.0980	38	92[d]
Solvent-free	0.05	0.1225	42	79[d]

[a] Reaction conditions: benzene (3 mmol), H_2O_2 (6 mmol), solvent-free, room temperature, reaction time = 1 h.
[b] mmol of Cr^{3+} in the used catalyst.
[c] Isolated yield.
[d] Determined by GC. The main byproduct was quinone.

Table III. Effect of Reaction Temperature on the Catalytic Activity of Fe_3O_4/MPA-PHEA-Cr[a]

Reaction temperature	Yield (%)[b]	Selectivity to phenol (%)[c]
Room temperature	31	100
35	39	87
45	43	75
65	40	70
Reflux	36	66

[a] Reaction temperature: benzene (3 mmol), catalyst (0.03 g), H_2O_2 (6 mmol), solvent-free, room temperature, reaction time = 1 h.
[b] Isolated yield.
[c] Determined by GC. The main byproduct was quinone.

In the view of industrial purposes, reusability of the catalyst was tested by carrying out repeated runs of the reaction on the same batch of the catalyst in the case of the model reaction (Table IV). In order to regenerate the catalyst, after each cycle, it was separated by an external magnet and washed several times with diethyl ether. Then, it was dried in an oven at 60°C and reused in the subsequent run. The results show that this polymer magnetic catalyst can be reused seven times with no significant loss of activity/selectivity performance. It should be mentioned that there was very low Cr^{3+} leaching during the reaction and the catalyst exhibited high stability even after seven recycles (Table IV).

Table IV. Reusability of the Catalyst[a]

Reaction cycles	Amount of Cr^{3+} (mmol/0.03 g catalyst)[b]	Yield (%)[c]
Fresh	0.0735	31
1	0.0731	31
2	0.0729	31
3	0.0724	29
4	0.0722	29
5	0.0721	28
6	0.0718	27
7	0.0714	26

[a] Reaction temperature: benzene (3 mmol), catalyst (0.03 g), H_2O_2 (6 mmol), solvent-free, room temperature, reaction time = 1 h, selectivity to phenol = 100%.
[b] Estimated by atomic absorption spectrometer.
[c] Isolated yield.

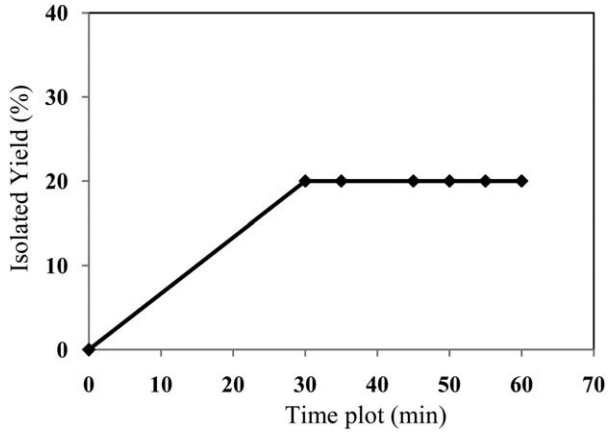

Figure 8. Heterogeneity test for hydroxylation of benzene over Fe_3O_4/MPA-PHEA-Cr.

In order to prove the heterogeneous nature of the catalyst, heterogeneity test was performed for the optimized hydroxylation benzene, in which the catalyst was separated from the reaction mixture at ~50% conversion of the starting material. The reaction progress in the filtrate was monitored. As displayed in Figure 8, no further hydroxylation reaction occurred even at extended times, indicating that the nature of reaction process is heterogeneous and there is not any reaction progress in homogeneous phase.

A comparative study was performed for the use of Fe_3O_4/MPA-PHEA-Cr with some of the reported catalysts for the hydroxylation of benzene (Table V). As can be observed, the reaction with different catalysts required a high temperature and longer reaction times compared with Fe_3O_4/MPA-PHEA-Cr. In all methods, the reaction was also performed in solvent such as acetonitrile and acetic acid. As mentioned earlier, when magnetic nanoparticles are generally used as supports, the size of the support materials is decreased to the nanometer scale, and all of the catalytic sites on the external surface of the particles can be accessible to the substrates.[7] Therefore, the nanometer scale polymer supported on the magnetic nanoparticle makes it an excellent scaffold for incorporation of chromium ions, leading to better dispersion of the active sites. As a consequence, the isolated active sites (Cr^{+3}) in the structure of the catalyst may be more reachable to benzene compared with the other catalytic systems, which causes the high catalytic activity in the hydroxylation of benzene. Furthermore, the high efficiency of this magnetic catalyst could be also due to the synergetic effect of Cr^{3+} ions and Lewis acidity of the Fe^{3+} groups in the structure of magnetic nanocomposite, which facilitate the formation of product intermediate.

CONCLUSION

In conclusion, a facile route to the synthesis of Cr(III)-containing Fe_3O_4/MPA-PHEA nanocomposite was reported without using any organosilane precursors. The magnetic nanoparticles were initially prepared by a simple co-precipitation in the presence of MPA to obtain Fe_3O_4/MPA. Then, the polymerization of HEA on the surface of Fe_3O_4/MPA was conducted through an *in situ* polymerization using AIBN as an initiator, which led to synthesize a new polymer-grafted magnetic nanoparticle (Fe_3O_4/MPA-PHEA). The surface functionalization of magnetic nanoparticles by MPA-PHEA was confirmed by several analytical apparatus. The instrumental analysis showed that immobilization of the polymer (PHEA) onto the modified magnetic nanoparticles (Fe_3O_4/MPA) was through the thiol groups of MPA, which resulted that the oxygen groups on the flexible supported polymer chain are effective at capturing chromium ions. The polymer-grafted magnetic nanoparticles containing Cr^{3+} exhibited high catalytic activity/selectivity in direct hydroxylation of benzene using hydrogen peroxide as green oxidant under mild conditions. The outstanding catalytic performance of this magnetic catalyst may be due to the synergetic effect between Cr^{3+} and Fe^{3+} groups in the structure of nanocomposite. The magnetic catalyst also showed high thermal stability and excellent level of reusability, which make it as a good candidate for industrial catalytic purposes in different oxidation reactions.

Table V. Hydroxylation of Benzene Using Hydrogen Peroxide over Different Catalysts

Entry	Catalyst	Time (h)	Yield (%)	Selectivity to phenol (%)	Temperature (°C)	Solvent	Ref.
1	Fe/MgO	6	36	100	60°C	Acetonitrile	32
2	Fe_3O_4/CMK-3	3	18	92	60°C	Acetonitrile	18
3	Multi-V-POMs	2	~25	~91	80°C	Acetonitrile	33
4	HPMoV/NH_2-SBA-15	6	20	95	60°C	Acetonitrile	34
5	P-[DVB-VBIM]$_5$PMoV_2	6	~24	100	55°C	Acetonitrile	35
6	Fe/MWCNTs	2.5	~18	~95	60°C	Acetonitrile	1
7	Poly(VMCA)-PMoV	4.5	~30	100	70°C	Acetonitrile	36
8	V-MimSalm-PMoV	5	~20	100	50°C	Acetonitrile	37
9	Co-SBA-16	4	~29	~97	70°C	Acetic acid	38
10	Fe_3O_4/MPA-PHEA-Cr	1	31	100	r.t	Solvent-free	This Work

ACKNOWLEDGMENTS

The authors thank the Isfahan Science and Technology Town (Isfahan University of Technology) for the support of this work. The authors also appreciate Dr. A. Heidarnejad for his helpful comments.

REFERENCES

1. Song, S.; Yang, H.; Rao, R.; Liu, H.; Zhang, A. *Appl. Catal. A* **2010**, *375*, 265.
2. Molinari, R.; Argurio, P.; Poerio, T. *Appl. Catal. A* **2012**, *437*, 131.
3. Tanarungsun, G.; Kiatkittipong, W.; Praserthdam, P.; Yamada, H.; Tagawa, T.; Assabumrungrat, S. *Catal. Commun.* **2008**, *9*, 1886.
4. Lemke, K.; Ehrich, H.; Lohse, U.; Berndt, H.; Jähnisch, K. *Appl. Catal. A* **2003**, *243*, 41.
5. Bianchi, D.; Bertoli, M.; Tassinari, R.; Ricci, M.; Vignola, R. *J. Mol. Catal. A* **2003**, *200*, 111.
6. Kumar, K. S.; Kumar, V. B.; Paik, P. *J. Nanopart.* **2013**, Article ID 672059, 24.
7. Phan, N. T. S.; Jones, C. W. *J. Mol. Catal. A* **2006**, *253*, 123.
8. Liu, G.; Hong, R. Y.; Guo, L.; Li, Y. G.; Li, H. Z. *Appl. Surf. Sci.* **2011**, *257*, 6711.
9. Liu, X. Q.; Guan, Y. P.; Ma, Z. Y.; Liu, H. Z. *Langmuir* **2004**, *20*, 10278.
10. Kara, A.; Erdem, B. *J. Mol. Catal. A* **2011**, *349*, 42.
11. Kawashita, M.; Tanaka, M.; Kokubo, T.; Inoue, Y.; Yao, T.; Hamada, S.; Shinjo, T. *Biomaterials* **2005**, *26*, 2231.
12. Li, B.; Gao, L.; Bian, F.; Yu, W. *Tetrahedron Lett.* **2013**, *54*, 1063.
13. Jin, X.; Zhang, K.; Sun, J.; Wang, J.; Dong, Z.; Li, R. *Catal. Commun.* **2012**, *26*, 199.
14. Feng, G.; Hub, D.; Yang, L.; Cui, Y.; Cui, X.; Li, H. *Sep. Purif. Technol.* **2010**, *74*, 253.
15. Esmaeilpour, M.; Sardarian, A. R.; Javidi, J. *Appl. Catal. A* **2012**, *445–446*, 359.
16. Ucoski, G. M.; Nunes, F. S.; DeFreitas-Silva, G.; Idemori, Y. M.; Nakagaki, S. *Appl. Catal. A* **2013**, *459*, 121.
17. Sirotin, S. V.; Moskovskaya, I. F. *Pet. Chem.* **2009**, *49*, 99.
18. Arab, P.; Badiei, A.; Koolivand, A.; Ziarani, G. M. *Chin. J. Catal.* **2011**, *32*, 258.
19. Zamani, F.; Rezapour, M.; Kianpour, S. *Bull. Korean Chem. Soc.* **2013**, *34*, 2367.
20. Zamani, F.; Izadi, E. *Catal. Commun.* **2013**, *42*, 104.
21. Zamani, F.; Izadi, E. *J. Inorg. Organomet. Polym.* **2013**, *23*, 1501.
22. Karaoğlu, E.; Baykal, A.; Senel, M.; Sözeri, H.; Toprak, M. S. *Mater. Res. Bull.* **2012**, *47*, 2480.
23. Kalbasi, R. J.; Massah, A. R.; Zamani, F.; Bain, A. D.; Breno, B. *J. Porous Mater.* **2011**, *18*, 475.
24. Cabrera, L.; Gutierrez, S.; Morales, M. P.; Menendez, N.; Herrasti, P. *J. Magn. Magn. Mater.* **2009**, *321*, 2115.
25. Deng, H.; Lei, Z. *Compos. B* **2013**, *54*, 194.
26. Zhang, L.; He, R.; Gu, H. C. *Appl. Surf. Sci.* **2006**, *253*, 2611.
27. Chen, A. Z.; Kang, Y. Q.; Pu, X. M.; Yin, G. F.; Li, Y.; Hu, J. Y. *J. Colloid Interface Sci.* **2009**, *330*, 317.
28. Manning, B.; Kiser, J.; Kwon, H.; Kanel, S. R. *Environ. Sci. Technol.* **2007**, *41*, 586.
29. Teranishi, T.; Miyake, M. *Chem. Mater.* **1998**, *10*, 594.
30. Parida, K. M.; Rath, D. *Appl. Catal. A* **2007**, *321*, 101.
31. Chammingkwan, P.; Hoelderich, W. F.; Mongkhonsi, T.; Kanchanawanichakul, P. *Appl. Catal. A* **2009**, *352*, 1.
32. Renuka, N. K. *J. Mol. Catal. A* **2010**, *316*, 126.
33. Yang, H.; Wu, Q.; Li, J.; Dai, W.; Zhang, H.; Lu, D.; Gao, S.; You, W. *Appl. Catal. A* **2013**, *457*, 21.
34. Kharat, A. N.; Moosavikia, S.; Jahromi, B. T.; Badiei, A. *J. Mol. Catal. A* **2011**, *348*, 14.
35. Zhao, P.; Leng, Y.; Wang, J. *Chem. Eng. J.* **2012**, *204–206*, 72.
36. Leng, Y.; Liu, J.; Jiang, P.; Wang, J. *Catal. Commun.* **2013**, *40*, 84.
37. Leng, Y.; Liu, J.; Jiang, P.; Wang, J. *Chem. Eng. J.* **2014**, *239*, 1.
38. Dong, Y.; Zhan, X.; Niu, X.; Li, J.; Yuan, F.; Zhu, Y.; Fu, H. *Micropor. Mesopor. Mater.* **2014**, *185*, 97.